

Robust Adaptive Observer for a Muscular Blood Vessel Fractional-Order Model [★]

Marcos A. González-Olvera ^{*} Ana G. Gallardo-Hernández ^{**}
Jesica Escobar ^{***}

^{*} *Universidad Autónoma de la Ciudad de México, Plantel San Lorenzo Tezonco. Mexico City, Mexico. (e-mail: marcos.angel.gonzalez@uacm.edu.mx).*

^{**} *Unidad de Investigacion Medica en Enfermedades Metabolicas, Instituto Mexicano del Seguro Social, Cuauhtemoc 330, 03400, Mexico, Mexico City, Mexico (e-mail: anagabygh@gmail.com)*

^{***} *Instituto Politécnico Nacional, ESIME Zacatenco. Mexico City, Mexico. (e-mail: jeazesme@hotmail.com)*

Abstract: Coronary disease modeling and prevention has proven critical to medical applications and patient evaluation. In this study, a robust observer for a fractional-order Muscular Blood Vessel (MBV) model that, using only measurements from the change in pressure, is proposed so it can reconstruct the change in the inner radius of the vessel. With this application, it is expected to provide a better prediction of future or present problems in the MBV. Parametric linear and nonlinear reconstruction, as well as state observation, is considered with noisy measurement cases. Numeric results are presented to demonstrate the capabilities of the proposed method.

Keywords: Fractional order systems, fractional difference equations, chaotic oscillator, robust observer.

1. INTRODUCTION

Adaptive systems design for fractional-order systems (FOS) is still an active research field, as several properties that have been common in integer-order adaptive systems do not extrapolate directly to the fractional-order case, beginning even from the concept of state itself (Sabatier et al., 2014). Several results on the study of adaptive systems rely on the analysis of time-varying nonlinear FOS, and explicit solutions have proven harder to obtain, compared to integer-order systems, except for counted cases (Eckert et al., 2019).

The problem of parameter identification has been of interest (Escobar et al., 2022), as it helps to obtain a more precise model for physical systems (Sabatier et al., 2006), or general nonlinear models (González-Olvera et al., 2015), and even with toolboxes for the case of linear systems that are already available for Matlab (Tepļakov et al., 2011). For on-line parameter and pseudo-state reconstruction, observer design for FOS has been addressed in recent works (Trigeassou et al., 2012; Balachandran et al., 2013), as well as the observer-based control design (N'Doye et al., 2009; Sheng et al., 2018). Some of the advances recently reported include

some classes of nonlinear FOS (Zhang and Gong, 2014), with an integer order adaptation law relying on \mathcal{H}_∞ by solving LMIs with an indirect Lyapunov method (N'Doye et al., 2017) and on-line least-squares algorithm for linear systems (Wei et al., 2015). In the last case, still integer-order adaptation laws are considered, and stability and convergence on-line is not obtained, particularly in the transient response. In recent works, an adaptive observer using Lyapunov analysis has been proposed (González-Olvera and Tang, 2018) and applied to biological systems (González-Olvera et al., 2021). However, there is still ongoing research for nonlinear fractional-order observer design, and generalizations of the fractional-order Kalman Filter (FKF) have been proposed Solís-Pérez et al. (2019), as well for the Extended FKF (EFKF) Sun et al. (2018), where still convergence conditions have to be studied.

In this sense, the application of fractional-order models has helped to better describe the long-term dynamic behaviour present in biological and biomedical systems (Rihan, 2013). For example, Djordjević et al. (2003) showed how fractional operators describe some rheological dynamics characteristics in cellular structures. One important medical application is the analysis of the chaotic pressure oscillations in the coronary artery in ischemic heart patients. The chaotic pressure is caused by extra and intracellular muscle Ca^{2+} fluxes in muscular

[★] M.A. González-Olvera wants to thank UACM for its financial support via Project UACM/CCyT/2022/13.

blood vessels (MBV) (Griffith and Edwards, 1994). Consequently, the vascular spasm behaviour, that is a form of a ischemic heart disease, can be seen mathematically as a chaotic state (Lin et al., 2012), and the drugs used to suppress the chaotic state, and turn it into a normal periodic orbit, like nitroglycerin, can be considered a control signal. As indicated by Magin (2010), fractional-order models have successfully described the elastic properties of blood vessels and arteries, as well as the energy absorption, validated by some experimental results with *in vivo* tissue Craiem and Armentano (2007). Therefore, a proper parameter identification and state observation can help to identify relevant dynamics and, in a future, personalize the medical treatment for heart diseases, that remains one of the leading death causes world-wide and imposes a big burden on health-care systems (Virani et al., 2020).

In this study, we render a multidisciplinary approach to help to improve the medical treatment for heart diseases, by proposing an observer and identification scheme based on an extension of a robust observer for fractional-order Muscular Blood Vessel model that, using only measurements from the change in pressure, can reconstruct, via an adapted EKF from Sun et al. (2018), the change in the inner radius of the vessel, and therefore help to better identify future or present problems in the MBV. Also, a parametric reconstruction is considered even in noisy measurement cases.

2. PROBLEM FORMULATION

2.1 Fractional-Order systems

Consider the SISO nonlinear fractional-order system given by

$${}_0D_t^\alpha \mathbf{x}(t) = \mathbf{f}(\mathbf{x}(t), t) \quad (1)$$

$$y = \mathbf{h}(\mathbf{x}) \quad (2)$$

The fractional Riemann-Liouville integral of order $\alpha \in (0, 1)$ is given by

$$I_0^\alpha \mathbf{x}(t) = \frac{1}{\Gamma(\alpha)} \int_0^t (t - \tau)^{\alpha-1} \mathbf{x}(\tau) d\tau \quad (3)$$

The fractional Caputo derivative of a function $\mathbf{f}(t)$ is defined by

$${}_0^C D_t^\alpha \mathbf{x}(t) = I_0^{\alpha-1} \frac{d\mathbf{x}(t)}{dt}, \quad (4)$$

and the fractional Riemann-Liouville derivative of a function $\mathbf{f}(t)$ is defined by

$${}_0^{\mathcal{R}\mathcal{L}} D_t^\alpha \mathbf{x}(t) = \frac{d}{dt} (I_0^{1-\alpha} \mathbf{x}(t)) \quad (5)$$

It is known that the Caputo and Riemann-Liouville derivatives are related, when $\alpha \in (0, 1)$, by

$${}_0^C D_t^\alpha \mathbf{x}(t) = {}_0^{\mathcal{R}\mathcal{L}} D_t^\alpha \mathbf{x}(t) - \frac{t^{1-\alpha}}{\Gamma(1-\alpha)} \mathbf{x}(0) \quad (6)$$

It is worth noticing that if initial conditions are zero, both derivatives converge to the same solution. However, this is not the case for the analysis of fractional-order dynamic systems, where initial conditions are not usually zero.

Also, it is known that the Riemann-Liouville derivatives can be obtained from the Grünwald-Letnikov definition, given by

$${}_0^{\mathcal{G}\mathcal{L}} D_t^\alpha \mathbf{x}(t) = \lim_{N \rightarrow \infty} \frac{1}{h_N^\alpha} \sum_{k=0}^N c(\alpha, k) \mathbf{x}(t - kh_N) \quad (7)$$

where $h_N = \frac{t}{N}$, $v(\alpha, k) = \frac{\Gamma(\alpha+1)}{\Gamma(\alpha-k+1)\Gamma(k+1)}$, $c(\alpha, k) = (-1)^k v(\alpha, k)$.

2.2 Muscular Blood Vessel Fractional-Order Model

In (Lin et al., 2012), the integer-order model for a Muscular Blood Vessel (MBV) has been described as

$$\dot{\mathbf{x}} = \begin{pmatrix} -bx_1 - cx_2 \\ -(1+b)\lambda x_1 - (1+c)\lambda x_2 + \lambda x_1^3 + I(\omega, t) \end{pmatrix}, \quad (8)$$

where the state x_1 models the change of the internal diameter of the blood vessel, x_2 is the pressure change in the vessel, $I(\omega, t)$ is a periodical stimulus, and b , c , λ are the system parameters. It has been described that a myocardial infarction can occur due to coronary atherosclerosis and/or a spasm in the coronary artery.

In (Gong et al., 2006; Aghababa and Borjkhani, 2014), the fractional-order model for a Muscular Blood Vessel (FOMBV) has been described by

$${}_0^C D_t^\alpha \mathbf{x} = \begin{pmatrix} -bx_1 - cx_2 \\ -(1+b)\lambda x_1 - (1+c)\lambda x_2 + \lambda x_1^3 + I \end{pmatrix}, \quad (9)$$

where $0 < \alpha < 1$ and $I = I(\omega, t)$.

In Fig. 1 it is shown how the change of the blood vessel internal diameter, as well as the change in pressure, change periodically when considering parameters $\alpha = 0.95$, $b = 0.15$, $c = -1.7$, $\lambda = -0.65$, $I(\omega, t) = 1.2 + 0.5 \cos(\omega(t)(t - t_f))\theta(t - t_f)$, where $\omega = 1.2$. However, if a sudden change in ω occurs (in this case, simulated at $t_f = 150$ in Fig. 1), the FOMBV enters into a chaotic behaviour.

3. MAIN RESULT

From Mendes et al. (2019), a numerical method in difference equations developed to consider the effect of the initial condition for (9) is then given by

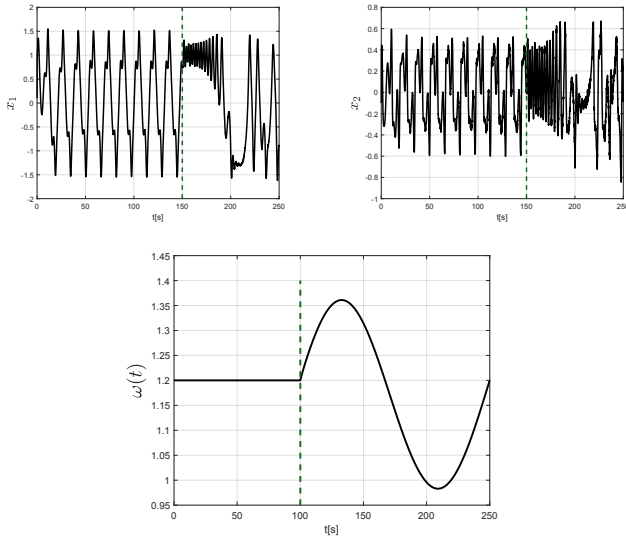


Fig. 1. Simulation of the FOMBV, considering a change in the nonlinear parameter of the external stimulus $\omega(t)$ in $I(\omega, t)$ at $t = 150$ s.

$$\mathbf{x}_{i+1} = h^\alpha \times \left(\begin{array}{c} -bx_1(ih) - cx_2(ih) \\ -(1+b)\lambda x_1(ih) - (1+c)\lambda x_2 + \lambda x_1^3 + I(\omega, ih) \end{array} \right) - \sum_{k=1}^{i+1} c(\alpha, k) \mathbf{x}(i-k+1) + \mathbf{x}(0) \left(1 + \sum_{k,i=1}^{i+1} c(\alpha, k) \right) \quad (10)$$

where $\mathbf{x}_i = \mathbf{x}(ih)$ and h is the time step of the numerical solution, *i.e.* $t = ih$.

Numerically, a fractional difference that updates the solution of the fractional-order differential equation can be seen as

$$\Delta^\alpha \mathbf{x}_{i+1} = h^\alpha \times \left(\begin{array}{c} -bx_1(ih) - cx_2(ih) \\ -(1+b)\lambda x_1(ih) - (1+c)\lambda x_2 + \lambda x_1^3 + I(\omega, ih) \end{array} \right) \triangleq \mathbf{f}_h(\mathbf{x}_i, ih) \quad (11)$$

and the update equation in discrete-time is given by

$$\mathbf{x}_{i+1} = \Delta^\alpha \mathbf{x}_{i+1} - \sum_{k=1}^{i+1} c(\alpha, i) \mathbf{x}_{i+1-k} \quad (12)$$

Considering that only the pressure change in the vessel can be measured, then the output depends linearly from the states, so it can be expressed by

$$y_i = C\mathbf{x}_i \quad (13)$$

where $C \in \mathbb{R}^{p \times n}$, where p is the number of outputs and n the number of pseudo-states.

3.1 Extended Fractional-Order Kalman Filter

From Sun et al. (2018), given (12), the EKF for a single output system can be obtained by

$$\hat{\mathbf{x}}_{i+1} = \mathbf{f}_h(\hat{\mathbf{x}}_i, ih) - \sum_{k=1}^{i+1} c(\alpha, k) \hat{\mathbf{x}}_{i+1-k} + (\mathbf{K}_i + \theta_i) (y_i - C\hat{\mathbf{x}}_i) + \hat{\mathbf{x}}(0) \left(1 + \sum_{k=1}^{i+1} c(\alpha, k) \right) \quad (14)$$

where δ is a design parameter, \mathbf{I} is the identity matrix, and

$$\begin{aligned} \mathbf{P}_{i+1} &= \mathbf{A}_i \mathbf{P}_i^T \mathbf{A}_i^T + \mathbf{Q}_i + \mathbf{D}_i \delta \mathbf{I} \\ &+ \mathbf{A}_i \mathbf{P}_i v(\alpha, 1) + \mathbf{P}_i \mathbf{A}_i^T v(\alpha, 1) \\ &+ \sum_{k=1}^{i+1} v(\alpha, k)^2 \mathbf{P}_{i+1-k} \\ &- (\mathbf{A}_i \mathbf{P}_i C^T + v(\alpha, 1) \mathbf{P}_i C^T) \times \\ &\mathbf{D}_i^{-1} \times (\mathbf{A}_i \mathbf{P}_i C^T + v(\alpha, 1) \mathbf{P}_i C^T)^T, \end{aligned} \quad (15)$$

$$\mathbf{K}_i = (\mathbf{A}_i \mathbf{P}_i C^T + v(\alpha, 1) \mathbf{P}_i C^T) \times \mathbf{D}_i^{-1}, \quad (16)$$

$$\mathbf{D}_i = C \mathbf{P}_i C^T + \mathbf{R}_i, \quad (17)$$

$$\mathbf{A}_i = \left. \frac{\partial \mathbf{f}_h(\mathbf{x}, t)}{\partial \mathbf{x}} \right|_{\mathbf{x}=\hat{\mathbf{x}}_i, t=hi} = h^\alpha \left. \frac{\partial \mathbf{f}(\mathbf{x}, t)}{\partial \mathbf{x}} \right|_{\mathbf{x}=\hat{\mathbf{x}}_i, t=hi}, \quad (18)$$

$$\mathbf{C}_i = \left. \frac{\partial \mathbf{h}(\mathbf{x})}{\partial \mathbf{x}} \right|_{\mathbf{x}=\hat{\mathbf{x}}_i}. \quad (19)$$

3.2 Observer and parametric reconstruction

If it is considered that only the change in blood pressure x_2 is measurable and the nonlinear term ω is unknown, then an augmented system is considered as

$$\begin{pmatrix} {}^C_0 D_t^\alpha x_1 \\ {}^C_0 D_t^\alpha x_2 \\ {}^C_0 D_t^\alpha \omega \end{pmatrix} = \begin{pmatrix} -bx_1 - cx_2 \\ -(1+b)\lambda x_1 - (1+c)\lambda x_2 + \lambda x_1^3 + I \\ 0 \end{pmatrix}, \quad (20)$$

then (14) can be used for the reconstruction of both x_1 and ω in $I = I(\omega, t)$.

4. NUMERICAL RESULTS

The method presented was used in system (20) to reconstruct state x_1 and the nonlinear parameter ω that changes in $t = 100$ s as depicted in Fig. 9, and the parameters reported in Section 2. The design parameters were chosen as $h = 0.05$ s, $\mathbf{Q}_i = 10^{-3} \mathbf{I}_{3 \times 3}$, $\mathbf{R}_i = 1$, $d = 10^{-4}$, $\mathbf{P}_0 = 10 \mathbf{I}_{3 \times 3}$, considering an output signal contaminated by noise $y_i = C\mathbf{x}_i + \nu(t)$, with $\mathcal{E}\{\nu(t)\} =$

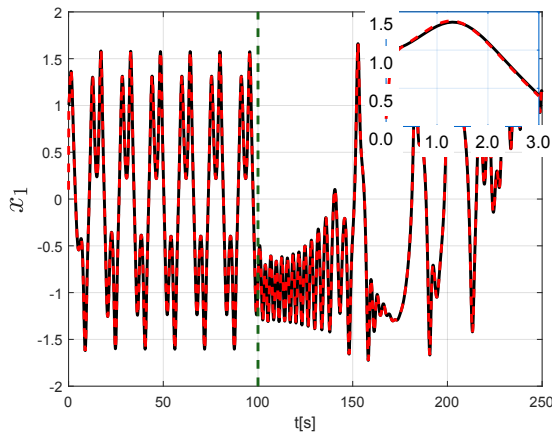


Fig. 2. Observer results for state x_1 . In solid line it is presented the state x_1 , while in red dashed line corresponds to the reconstructed state \hat{x}_1 .

$0, \mathcal{E}\{\nu^2(t)\} = 10^{-4}$. In Fig. 2,3 and 4 it can be seen how the proposed extended Kalman filter for the fractional case does achieve state and parameter reconstruction, even after the change in the nonlinear parameter ω happens, and how the chaotic behaviour is reconstructed by the observer itself. In general, it can be seen how the error effectively tends to zero, as shown in Fig. 5,6 and 7.

Moreover, it was also considered, as an extension, that also the parameter b is unknown under the same circumstances. In this case, the extended system is now:

$$\begin{pmatrix} {}^c_0D_t^\alpha x_1 \\ {}^c_0D_t^\alpha x_2 \\ {}^c_0D_t^\alpha \omega \\ {}^c_0D_t^\alpha b \end{pmatrix} = \begin{pmatrix} -bx_1 - cx_2 \\ -(1+b)\lambda x_1 - (1+c)\lambda x_2 + \lambda x_1^3 + I(\omega, t) \\ 0 \\ 0 \end{pmatrix}. \quad (21)$$

In this case, design parameters were chosen as $h = 0.05$ s, $\mathbf{Q}_i = 10^{-5}\mathbf{I}_{4 \times 4}$, $\mathbf{R}_i = 0.1$, $d = 10^{-5}$, $\mathbf{P}_0 = 10\mathbf{I}_{4 \times 4}$. Results are shown in Fig. 8 and 9, where it can be seen how there is state convergence, while the reconstructed parameters tend to a vicinity of the actual values.

5. CONCLUSIONS

A fractional-order extended Kalman filter for a fractional-order Muscular Blood Vessel (MBV) model was presented in this work. It was shown how, using only measurements from the change in arterial blood pressure, it can reconstruct the change in the inner radius of the vessel along with a linear and a nonlinear parameter of the model. However, it is still to be described the observability of the remaining parameters for the nonlinear model of the MBV, as well as the analytical stability properties of the proposed method. Nevertheless, this application is expected to aid with a better prediction and description of non desired dynamics in the MBV.

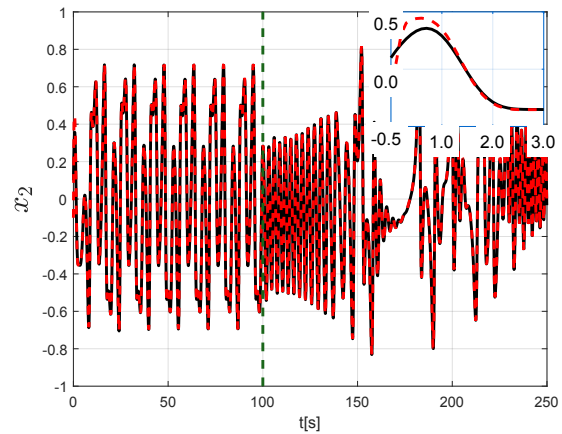


Fig. 3. Observer results for state x_2 . In solid line it is presented the state x_2 , while in red dashed line corresponds to the reconstructed state \hat{x}_2 .

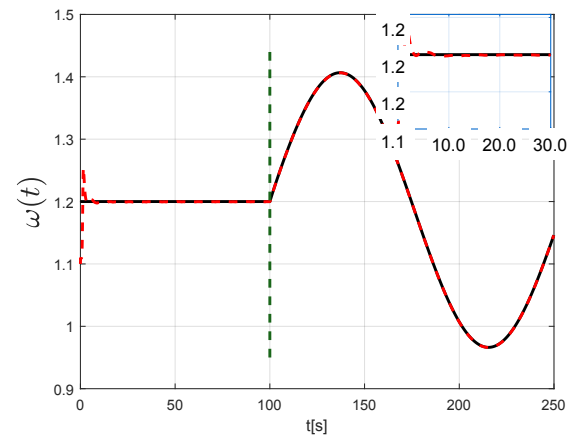


Fig. 4. Observer results for time-varying parameter ω . In solid line it is presented the value of ω , while in red dashed line corresponds to the reconstructed value for $\hat{\omega}$.

ACKNOWLEDGEMENTS

M.A. González-Olvera wants to thank UACM for its financial support via Project UACM/CCyT/2022/13.

REFERENCES

- Aghababa, M.P. and Borjkhani, M. (2014). Chaotic fractional-order model for muscular blood vessel and its control via fractional control scheme. *Complexity*, 20, 37–46. doi:10.1002/cplx.21502.
- Balachandran, K., Govindaraj, V., Rivero, M., Tenreiro Machado, J.A., and Trujillo, J.J. (2013). Observability of nonlinear fractional dynamical systems. *Abstract and Applied Analysis*, 2013(2). doi:10.1155/2013/346041.
- Craiem, D. and Armentano, R.L. (2007). A fractional derivative model to describe arterial viscoelasticity. *Biorheology*, 44(4), 251–263.

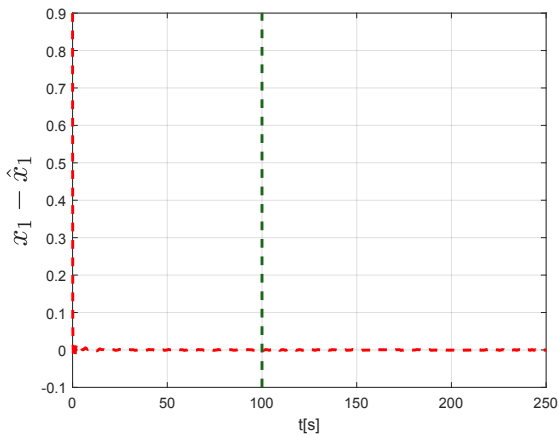


Fig. 5. Error results for state observation x_1

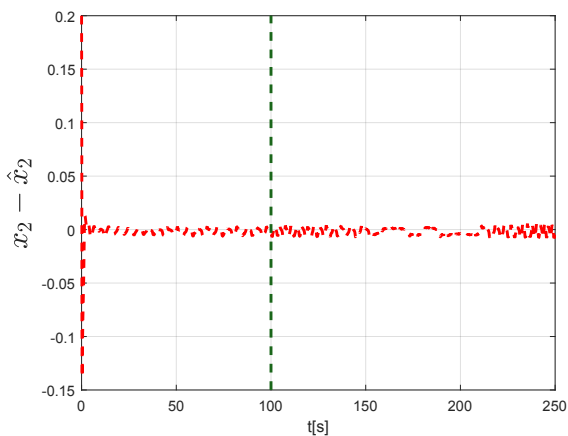


Fig. 6. Error results for state observation x_2

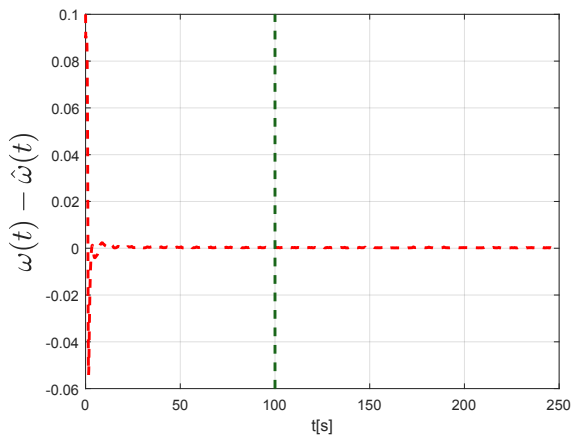


Fig. 7. Estimation error for time-varying parameter ω

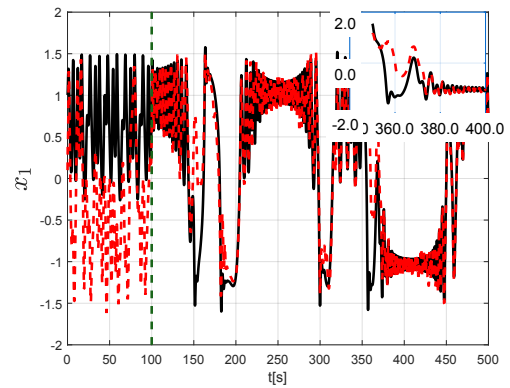


Fig. 8. Results for state observation x_1 for the joint estimation of parameters ω and b . The solid black line corresponds to the real value, while the dotted one to the one estimated by the EKF.

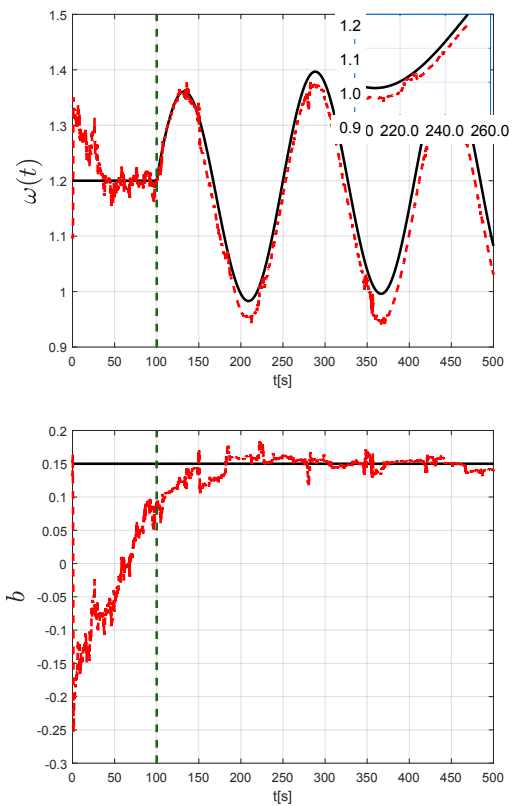


Fig. 9. Results for the joint estimation of parameters ω and b . The solid black line corresponds to the real value, while the dotted one to the one estimated by the EKF.

Djordjević, V.D., Jarić, J., Fabry, B., Fredberg, J.J., and Stamenović, D. (2003). Fractional derivatives embody essential features of cell rheological behavior. *Annals of biomedical engineering*, 31(6), 692–699.

- Eckert, M., Nagatou, K., Rey, F., Stark, O., and Hohmann, S. (2019). Solution of time-variant fractional differential equations with a generalized peano-baker series. *IEEE Control Systems Letters*, 3(1), 79–84. doi: 10.1109/LCSYS.2018.2852600.
- Escobar, J., Gallardo-Hernandez, A.G., and Gonzalez-Olvera, M.A. (2022). How to deal with parameter estimation in continuous-time stochastic systems. *Circuits, Systems, and Signal Processing*, 41(4), 2338–2357.
- Gong, C., Li, Y., and Sun, X. (2006). Backstepping control of synchronization for biomathematical model of muscular blood vessel. *Journal of Applied Sciences*, 24(6), 604–607.
- González-Olvera, M.A., Flores-Pérez, A., and Torres, L. (2021). Adaptive observer design for the fractional-order hindmarsh-rose neuron model. Asociación de México de Control Automático.
- González-Olvera, M.A. and Tang, Y. (2018). Adaptive observer for a class of nonlinear fractional-order systems. In *Congreso Nacional de Control Automático 2018*. Asociación de México de Control Automático.
- González-Olvera, M.A., Tang, Y., and Navarro-Guerrero, G. (2015). Fractional order system identification by a genetic algorithm. In *Memorias del Congreso Nacional de Control Automático*, 304–308.
- Griffith, T. and Edwards, D.H. (1994). Fractal analysis of role of smooth muscle ca^{2+} fluxes in genesis of chaotic arterial pressure oscillations. *American Journal of Physiology-Heart and Circulatory Physiology*, 266(5), H1801–H1811.
- Lin, C.J., Yang, S.K., and Yau, H.T. (2012). Chaos suppression control of a coronary artery system with uncertainties by using variable structure control. *Computers & Mathematics with Applications*, 64(5), 988–995. doi:https://doi.org/10.1016/j.camwa.2012.03.007. URL <https://www.sciencedirect.com/science/article/pii/S089812211200212X>.
- Advanced Technologies in Computer, Consumer and Control.
- Magin, R.L. (2010). Fractional calculus models of complex dynamics in biological tissues. *Computers & Mathematics with Applications*, 59(5), 1586–1593. doi: https://doi.org/10.1016/j.camwa.2009.08.039. Fractional Differentiation and Its Applications.
- Mendes, E.M., Salgado, G.H., and Aguirre, L.A. (2019). Numerical solution of caputo fractional differential equations with infinity memory effect at initial condition. *Communications in Nonlinear Science and Numerical Simulation*, 69, 237–247.
- N'Doye, I., Laleg-Kirati, T.M., Darouach, M., and Voos, H. (2017). H_∞ Adaptive observer for nonlinear fractional-order systems. *International Journal of Adaptive Control and Signal Processing*, 31(3), 314–331. doi:10.1002/acs.2699. URL <http://doi.wiley.com/10.1002/acs.2699>.
- N'Doye, I., Zasadzinski, M., Darouach, M., and Radhy, N.E. (2009). Observer-based control for fractional-order continuous-time systems. *Proceedings of the IEEE Conference on Decision and Control*, (1), 1932–1937. doi:10.1109/CDC.2009.5400443.
- Rihan, F.A. (2013). Numerical modeling of fractional-order biological systems. In *Abstract and Applied Analysis*, volume 2013. Hindawi.
- Sabatier, J., Aoun, M., Oustaloup, A., Grégoire, G., Ragot, F., and Roy, P. (2006). Fractional system identification for lead acid battery state of charge estimation. *Signal Processing*, 86(10), 2645–2657. doi:https://doi.org/10.1016/j.sigpro.2006.02.030. URL <https://www.sciencedirect.com/science/article/pii/S0165168406000533>. Special Section: Fractional Calculus Applications in Signals and Systems.
- Sabatier, J., Farges, C., and Trigeassou, J.C. (2014). Fractional systems state space description: Some wrong ideas and proposed solutions. *JVC/Journal of Vibration and Control*, 20(7), 1076–1084. doi: 10.1177/1077546313481839.
- Sheng, D., Wei, Y., Cheng, S., and Wang, Y. (2018). Observer-based adaptive backstepping control for fractional order systems with input saturation. *ISA Transactions*, 82, 18–29. doi:10.1016/j.isatra.2017.06.021. URL <http://dx.doi.org/10.1016/j.isatra.2017.06.021>.
- Solís-Pérez, J., Gómez-Aguilar, J., Torres, L., Escobar-Jiménez, R., and Reyes-Reyes, J. (2019). Fitting of experimental data using a fractional kalman-like observer. *ISA transactions*, 88, 153–169.
- Sun, Y., Wang, Y., Wu, X., and Hu, Y. (2018). Robust extended fractional kalman filter for nonlinear fractional system with missing measurements. *Journal of the Franklin Institute*, 355(1), 361–380.
- Tepljakov, A., Petlenkov, E., and Belikov, J. (2011). Fomcom: a matlab toolbox for fractional-order system identification and control. *International Journal of Microelectronics and computer science*, 2(2), 51–62.
- Trigeassou, J.C., Maamri, N., Sabatier, J., and Oustaloup, A. (2012). State variables and transients of fractional order differential systems. *Computers and Mathematics with Applications*, 64(10), 3117–3140. doi:10.1016/j.camwa.2012.03.099. URL <http://dx.doi.org/10.1016/j.camwa.2012.03.099>.
- Virani, S.S., Alonso, A., Benjamin, E.J., Bittencourt, M.S., Callaway, C.W., Carmon, A.P., Chamberlain, A.M., Chang, A.R., Cheng, S., Delling, F.N., et al. (2020). Heart disease and stroke statistics—2020 update: a report from the american heart association. *Circulation*, 141(9), e139–e596.
- Wei, Y.H., Sun, Z.Y., Hu, Y.S., and Wang, Y. (2015). On fractional order adaptive observer. *International Journal of Automation and Computing*, 12(6), 664–670. doi:10.1007/s11633-015-0929-3. URL <http://link.springer.com/10.1007/s11633-015-0929-3>.
- Zhang, R. and Gong, J. (2014). Synchronization of the fractional-order chaotic system via adaptive observer. *Systems Science and Control Engineering*, 2(1), 751–754. doi:10.1080/21642583.2014.891955.